BER Performance of Multibeam Satellite Systems with Tomlinson-Harashima Precoding

Mario Poggioni, Matteo Berioli, and Paolo Banelli

***Abstract*—A multibeam satellite system can be modelled as a multiple-input multiple-output (MIMO) system with an inter-beam interference matrix that is derived from the positions of the users in the different beams. This way it is possible to apply precoding techniques, such as Tomlinson-Harashima precoding (THP), to mitigate the interference. This paper presents an analytical framework to model the interference by a simple and effective parameter, which enables to assess the uncoded bit error rate (BER) of THP in such a scenario, and to derive useful hints on the optimization of the overall system capacity.**

***Index Terms*—Satellite, Interference, Precoding, THP, DVB-S2.**

I. Introduction

Large satellites built and launched in the last few years quite always employ multiple spotbeams, which allow to exploit more efficiently satellite resources at the price of more complex antenna systems. Indeed, the emission pattern of on-board antennas enables to confine the transmitted power on each frequency to a limited region of the Earth surface, and thus to reuse the same frequency to transmit on different beams. This way, these satellite systems exploit the *frequency reuse* concept employed also in cellular systems: beams characterized by different frequencies are organized in *clusters* [1], in such a way that beams in the same frequency are spaced as far as possible in order to reduce the co-channel interference (CCI). However, the residual CCI still represents the effect that limits the capacity in this type of systems.

Many techniques, mainly developed for terrestrial systems, and applied at either the receiver or the transmitter or both, can reduce or almost eliminate the CCI [2] [3]. In order to eliminate the CCI at the receiver as proposed in [4] by an iterative cancellation approach, the receiver complexity and cost are highly increased. As a consequence, many efforts have been made to move the CCI cancellation at the transmitter side, where the impact of signal processing costs is much lower [5]. In this view, information theory results have shown that the link capacity with interference is the same as in absence of interference, provided that this is perfectly known to the transmitter [6], and can be exploited by means of dirty-paper coding (DPC).

Unfortunately, transposing the theoretical results of Costa into practical systems is very difficult. Indeed, finding out the optimal precoding technique, which achieves the DPC capacity, is proven to be a non polynomial (NP) hard problem, i.e. with unmanageable complexity. On the other hand, simpler linear precoding (LP) techniques [7], with manageable complexity, generally produce considerable performance degradation. Tomlinson-Harashima precoding (THP) is a simple although effective technique for eliminating CCI with only a limited increase in complexity with respect to LP. Originally developed to eliminate inter-symbol interference (ISI) in channels with memory, THP has been recently applied successfully to multiple-input multiple-output (MIMO) channels precoding [8], with a mathematical framework that can be exploited also for multibeam satellite systems simply replacing the channel matrix with the inter-beam interference matrix [9]. Basically, THP eliminates most of the transmission power increase of LP resorting to a modulo operation [5], both at the transmitter and the receiver side, which permits a perfect reconstruction of the information signal (in absence of noise). Thus, the use of THP in multibeam satellite systems to limit the inter-beam interference, which translates in a reduction of the beam cluster size and of the bandwidth usage per beam, globally produces an increase of the overall system capacity. In this work we show how the performance of this precoding technique is closely related to the characteristics of the inter-beam interference matrix, which in turn depends on the positions of the users on the ground. Specifically, we define a simple framework to analytically model the impact of the interference matrix characteristics on the BER performance of state-of-the art precoding techniques and we compare the throughput of precoded systems and clustered systems in the presence of CCI. This allows us to assess gains and drawbacks induced by precoding in a simple but effective way, which can be used to design multibeam satellite systems.

The rest of the paper is organized as follows. Section II describes the scenario and the THP considered in our analysis, while Section III discusses the importance of the users position for the precoder performance. In Section IV the throughput obtained with clustering and precoding (for different users placements) are compared and simulation results are presented in Section V. Finally, some conclusions are drawn in Section VI.

II. Scenario and Background

A. System model

We consider a multibeam broadband satellite system affected by CCI. Specifically, we focus on the forward link of a practical geostationary satellite system [10] for broadcasting, which works in the K-band (20 Ghz) and is located over Europe at 19° E.

This satellite covers its own area by employing 96 adjacent spot beams. Specifically, we will concentrate on two scenarios where $K = 10$ beams are organized according either to a cluster size $n_C = 1$ (Fig. 1) or $n_C = 3$ (Fig. 2).

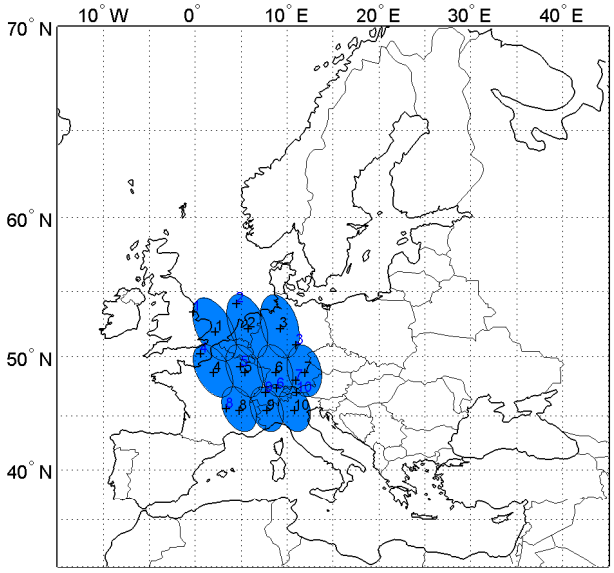

Fig. 1. Position of the beams for cluster size 1.

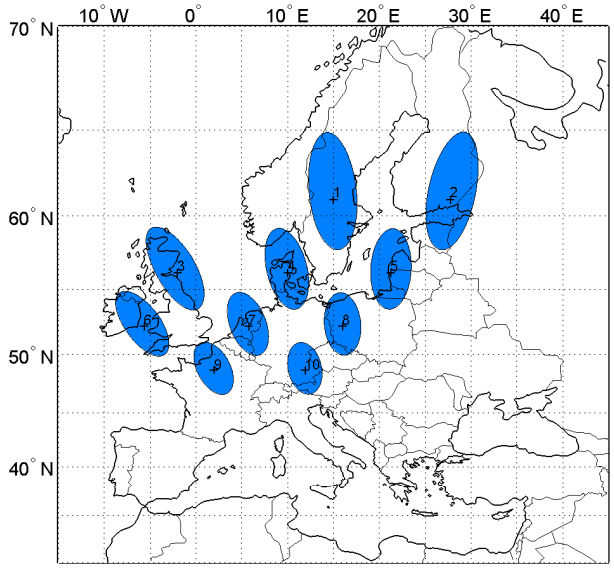

Fig. 2. Position of the beams for cluster size 3.

Both the scenarios correspond to a broadcast MIMO channel, with a unique transmitter that sends K independent information streams to K independent receivers, located in K different main beams, which suffer the interference from the other $K-1$ beam sidelobs. Mathematically, this is represented by a $K \times K$ *interference matrix* $\mathbf{H}$ that has on the (i,j)-th element $H_{i,j}$ (the square ratio of) the power of the j-th beam received by the i-th receiver, normalized by (the square ratio of) the power of the j-th beam on its own receiver [1].

In the following, we will indicate with $A_{i,j}$ the (i,j)-th element of a matrix $\mathbf{A}$ and with a_i the i-th element of a vector $\mathbf{a}$, and with $\Re\mathbf{a}$, $\Im\mathbf{a}$ the real and imaginary parts of $\mathbf{a}$.

In order to cope with CCI, the transmitter can modify the Quadrature Amplitude Modulation (QAM) modulated information vector $\mathbf{x}$ to be transmitted to the K users, in such a way to compensate the effect of the CCI. In a matricial form this is expressed by

$$\mathbf{y} = f(\mathbf{x}), \;\; g(\mathbf{H}\mathbf{y}) = \mathbf{x}, \tag{1}$$

where $\mathbf{y}$ is the transmitted signal, while $f(\cdot)$ and $g(\cdot)$ are suitable functions that eliminate the CCI at the transmitter and at the receiver, respectively. The received signal $\mathbf{z}$ is consequently expressed by

$$\mathbf{z} = \mathbf{H}\mathbf{y} + \mathbf{n}, \tag{2}$$

where the vector $\mathbf{n}$ is the thermal noise and the estimated signal $g(\mathbf{z}) = \mathbf{x} + \tilde{\mathbf{n}}$ is affected by a noise vector $\tilde{\mathbf{n}}$ obtained by a transformation of the random vector $\mathbf{n}$.

B. Tomlinson-Harashima Precoding

A very simple way to eliminate CCI is linear precoding (LP), which is accomplished, in a vector-matrix notation, by premultiplying the transmitted vector $\mathbf{x}$ by the Moore-Penrose pseudo-inverse of $\mathbf{H}$. However, this LP designed by means of a zero-forcing (ZF) approach, that is $\mathbf{y}_{\mathrm{LP}} = \mathbf{H}^{\dagger}\mathbf{x}$, induces a large waste of power at the transmitter when $\mathbf{H}$ is ill conditioned [7].

In order to counteract this drawback, Tomlinson-Harashima Precoding (THP) has been introduced [11] [12]. The main idea underlying THP is to constrain the transmitted power by replacing the QAM-modulated signal $\mathbf{x}$ with a suitable signal that is equivalent to $\mathbf{x}$ after the decoding at the receiver but requires less power to be transmitted after precoding. Specifically, THP exploits the mathematical concept of lattice by partitioning the $\mathbb{C}$ complex plane in a square *lattice* and by establishing an equivalence among the elements of this lattice. Specifically, a modulo operation is employed both at the transmitter and at the receiver in order to constrain each component of the complex vector generated in the precoding in a square centered in the origin of the complex plane with side $S = 4\sqrt{M}/\sqrt{2(M-1)/3}$, where M is the QAM constellation size, maintaining the position they had with respect to the centers of their own squares within the lattice[13]. This operation can be written, for each dimension, as

$$\mathrm{MOD}_M(x) = x - 2\sqrt{M}\left\lfloor \frac{x-\sqrt{M}}{2\sqrt{M}} \right\rfloor. \tag{3}$$

This way the power of the transmitted signal is kept below a certain value. Actually, the modulo operation is equivalent to add to a suitable transformation of the vector $\mathbf{x}$ a complex vector $\mathbf{d} \in (S\mathbb{Z})^K \times (S\mathbb{Z})^K$, as we will detail below. In order to make possible the decoding at the receiver with the same modulo operation it is necessary that this corresponds to add a complex vector $\tilde{\mathbf{d}} \in (S\mathbb{Z})^K \times (S\mathbb{Z})^K$ to the LP received signal $\mathbf{z} = \mathbf{x} + \mathbf{n}$.

Summarizing, THP can be viewed as a LP where $\mathbf{x}$ is replaced by $\mathbf{v} = \mathbf{x} + \tilde{\mathbf{d}}$, such that

$$\mathrm{MOD}_M(\Re(\mathbf{H}\mathbf{H}^\dagger(\mathbf{x}+\tilde{\mathbf{d}}))) = \mathrm{MOD}_M(\Re(\mathbf{x}+\tilde{\mathbf{d}})) = \Re\mathbf{x},$$
$$\mathrm{MOD}_M(\Im(\mathbf{H}\mathbf{H}^\dagger(\mathbf{x}+\tilde{\mathbf{d}}))) = \mathrm{MOD}_M(\Im(\mathbf{x}+\tilde{\mathbf{d}})) = \Im\mathbf{x}. \quad (4)$$

The goal of THP in order to minimize the transmitted power is to solve the minimization problem

$$\arg\min_{\mathbf{v}\in(S\mathbb{Z})^K\times(S\mathbb{Z})^K} \|\mathbf{y}\|^2, \quad (5)$$

where $\mathbf{y} = \mathbf{H}^\dagger\mathbf{v}$ is the transmitted signal.

Unfortunately, this problem is known to be NP-hard [14], and thus is necessary to resort to some sub-optimal approach.

In the following we will briefly explain how THP works by recasting state of the art precoding techniques. In order to exploit the modulo operation, the channel inversion is partially accomplished in a recursive fashion by means of a feedback matrix $\mathbf{B}$, which is strictly lower-triangular, with a null main diagonal, and such that $\mathbf{H}^\dagger = \mathbf{F}\mathbf{C}^{-1}\mathbf{Z}$, where $\mathbf{C} = \mathbf{I} + \mathbf{B}$. $\mathbf{F}$ and $\mathbf{Z}$ are the matrices that complete the inversion of $\mathbf{H}$ and should be chosen minimizing the eigenvalues of $\mathbf{F}$. In fact THP reduces the power of the transmitted signal $\mathbf{y}$ by constraining the power of the signal vector $\mathbf{b}$ (generated before the forward matrix $\mathbf{F}$), whose elements are calculated as

$$b_k = a_k - \sum_{j=1}^{k-1} B_{k,j}b_j + d_k, \quad (6)$$

where $\mathbf{a} = \mathbf{Z}\mathbf{x}$ and d_k is the element of the lattice $\mathbb{L}$ that minimizes the power of b_k by placing it in $[-S/2, S/2] \times [-S/2, S/2]$. It is worth noting that $d_1 = 0$ and $b_1 = a_1$. The vector $\mathbf{b}$ is consequently

$$\mathbf{b} = \mathbf{C}^{-1}(\mathbf{a}+\mathbf{d}) = \mathbf{C}^{-1}\mathbf{Z}(\mathbf{x}+\tilde{\mathbf{d}}), \quad (7)$$

which shows the equivalence of THP with a LP calculated on suitable points of the lattice $\mathbb{L}$.

The design of the matrices $\mathbf{F}$ and $\mathbf{Z}$ can be obtained with affordable complexity using the so-called Lattice Reduction Aided (LRA) precoding [15], which exploits a particular factorization of the matrix $\mathbf{H}$. Specifically, in order to exploit LRA, (2) is rewritten as

$$\mathbf{z}_r = \begin{bmatrix} \Re\mathbf{z} \\ \Im\mathbf{z} \end{bmatrix} = \begin{bmatrix} \Re\mathbf{H} & -\Im\mathbf{H} \\ \Im\mathbf{H} & \Re\mathbf{H} \end{bmatrix} \begin{bmatrix} \Re\mathbf{y} \\ \Im\mathbf{y} \end{bmatrix} + \begin{bmatrix} \Re\mathbf{n} \\ \Im\mathbf{n} \end{bmatrix} = \mathbf{H}_r \begin{bmatrix} \Re\mathbf{y} \\ \Im\mathbf{y} \end{bmatrix} + \begin{bmatrix} \Re\mathbf{n} \\ \Im\mathbf{n} \end{bmatrix} = \mathbf{H}_r\mathbf{y}_r + \mathbf{n}_r, \quad (8)$$

where the subscript *r* indicates the real-form of a complex vector or matrix as in (8). This way, in order to minimize the power of $\mathbf{y}_r$, the Lenstra-Lenstra-Lovasz (LLL) algorithm [16] is used to derive the factorization

$$\mathbf{H}_r = \mathbf{R}\mathbf{W}^H\mathbf{Q}, \quad (9)$$

where $\mathbf{R}$ is an *integer* matrix, $\mathbf{W}$ is the LLL-reduced basis matrix and $\mathbf{Q}$ is a suitable *unitary* matrix which accounts also for the ordering of the users that guarantees the best performance [9]. It is worth noting that $\mathbf{W}$ is *strictly lower triangular* and is *nearly unitary*.

Such a factorization corresponds to a THP where

$$\mathbf{H}_r^\dagger(\mathbf{x_r}+\mathbf{d_r}) = \mathbf{F}_r\mathbf{C}_r^{-1}\mathbf{Z}_r(\mathbf{x_r}+\mathbf{d_r}), \quad (10)$$

with $\mathbf{C}_r = \mathbf{W}\mathbf{D}$, $\mathbf{F}_r = \mathbf{Q}^H\mathbf{D}$ and $\mathbf{Z}_r = \mathbf{R}^H$.

Noteworthy, the matrix $\mathbf{Q}$ is unitary, thus the power increase at the transmitter caused by the forward matrix $\mathbf{F}_r$ premultiplication only depends on the diagonal matrix $\mathbf{D}$. Consequently, we can evaluate the SNR reduction caused by the inversion of $\mathbf{H}$ as

$$g_{\mathrm{LLL}} = \frac{\mathrm{SNR}_R}{\mathrm{SNR}_T} = \frac{12K}{S^2\sum_{k=1}^{2K}\frac{1}{|W_{k,k}|^2}}, \quad (11)$$

where SNR_R and SNR_T are the SNR at the receiver and at the transmitter, respectively, while $D_{k,k} = 1/W_{k,k}, \forall k$ and the term $12/S^2$ accounts for the fact that the elements of $\mathbf{b}_r$ are roughly uniformly distributed in $[-S/2, S/2]$ [17].

With the LLL algorithm the THP does not act on $\mathbf{x_r}+\tilde{\mathbf{d}}_\mathbf{r}$ but on $\mathbf{a}_r+\mathbf{d_r} = \mathbf{R}^H(\mathbf{x_r}+\tilde{\mathbf{d}}_\mathbf{r})$. It is worth noting that the receiver can successfully decode the signal $\mathbf{z_r} = \mathbf{H}_r\mathbf{F}_r\mathbf{C}_r^{-1}(\mathbf{x_r}+\tilde{\mathbf{d}}_\mathbf{r})+\mathbf{n_r}$, because $\mathbf{Z}^{-1} = (\mathbf{R}^H)^{-1}$ is an integer matrix and $\tilde{\mathbf{d}}_\mathbf{r} = (\mathbf{R}^H)^{-1}\mathbf{d_r}$ is still a point of the lattice $\mathbb{L}$. Since the matrix $\mathbf{W}$ is nearly unitary, the SNR degradation g_{LLL} is limited with respect to other possible factorizations of $\mathbf{H}$ such as the Cholesky factorization [13], where $\mathbf{Z} = \mathbf{I}$.

Even if LRA precoding is not optimum, known methods that can outperform it have a much higher complexity and can be impractical for a high K [15]. As a consequence, in the following we will consider LRA precoding as a reference for our analysis of the BER performance of LRA THP.

C. Theoretical BER Estimation for THP

We have assessed above the SNR degradation induced by LRA THP. However, BER performance is affected also by the modulo operation that the receiver has to perform to recover the transmitted signal. In fact, *even if the CCI is perfectly cancelled*, the noise at the receiver can cause a wrong estimation of the vector $\tilde{\mathbf{d}}$. This corresponds to have several replicas of the M-QAM constellation on the $\mathbb{R}^2$ plane, with an enhanced SER.

For the general M-QAM case the uncoded BER performance of THP is readily assessed if we note that, because of the modulo operation, all the symbols have four neighbors, while in the AWGN case this does not hold true for the symbols on the borders of the constellation. Therefore, when modulo operation is applied all the symbols have the same SER (and, with Gray coding, the same BER), thus the THP uncoded BER is obtained by removing the term $1 - 1/\sqrt{M}$ (which accounts for the different SER of the symbols on the borders of the constellation) from the well-known AWGN BER expressions [18]:

$$BER_{\mathrm{LLL}} = 1 - (1 - \tilde{P}_{\mathrm{SC}})^2, \quad (12)$$

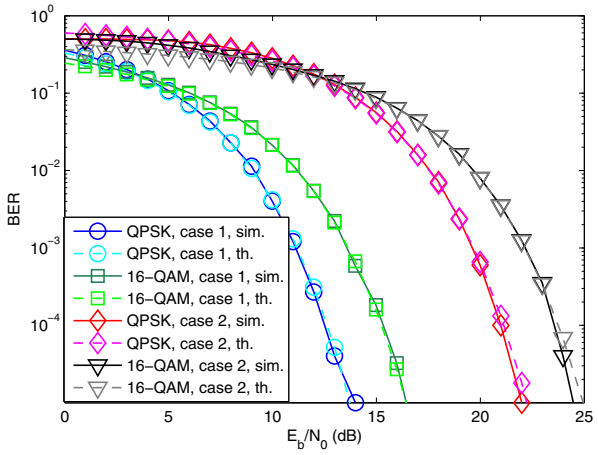

Fig. 3. Simulated and theoretical uncoded BER for different scenarios.

$$\tilde{P}_{\mathrm{SC}} = \frac{2}{k} Q\left(\sqrt{\frac{3k}{M-1} g_{\mathrm{LLL}} \frac{E_b}{N_0}}\right), \tag{13}$$

where $k = \log_2(M)$ is the number of bits per symbol and g_{LLL} is the SNR degradation in (11).

We show in Fig. 3 the almost perfect match between simulated and theoretical THP uncoded BER for QPSK and 16-QAM, and for two interference matrices corresponding to a moderate (case 1) and a high (case 2) CCI, respectively. Thus, assuming that the CCI is perfectly cancelled, it is possible to predict very well the uncoded BER experienced by a THP system by means of the sole g_{LLL} parameter.

III. Interference Modelling

As explained in the previous Section, the BER performance of THP is strictly related to the characteristics of the interference matrix $\mathbf{H}$ and to its specific factorization. Specifically, we have shown that the performance of LRA THP depends on the single parameter g_{LLL}, which is the sum of the absolute values of the reciprocal of the entries on the diagonal of the LLL-reduced basis $\mathbf{W}$, as shown in (11). Although a mathematical relation between this parameter and the positions of the receivers in their beams cannot be easily derived, it is clear that when two or more users are very close g_{LLL} usually assumes a lower value, i.e., the more the CCI, the more the SNR degradation for the precoding.

In order to have a meaningful assessment of the effect of users' positioning on THP precoding, we generated 1000 sets of users uniformly placed on the $K = 10$ beams shown in Fig. 1. Then, for each set, we computed the interference matrix $\mathbf{H}$ and the associated LLL-reduced basis $\mathbf{W}$. We plot in Fig. 4 an histogram of the values of $\sum_{k=1}^{K} |1/W_{k,k}|^2$ assumed by each users' set. It is evident that in most cases the LRA precoding is able to reduce the SNR degradation g_{LLL} to acceptable values (around 2 dB), although in some cases it can still be very high (up to 12 dB). Interestingly, we found a correlation coefficient $\rho = 0.8$ between the values of $1/g_{\mathrm{LLL}}$ and $1/d_{\mathrm{MIN}}$, where,

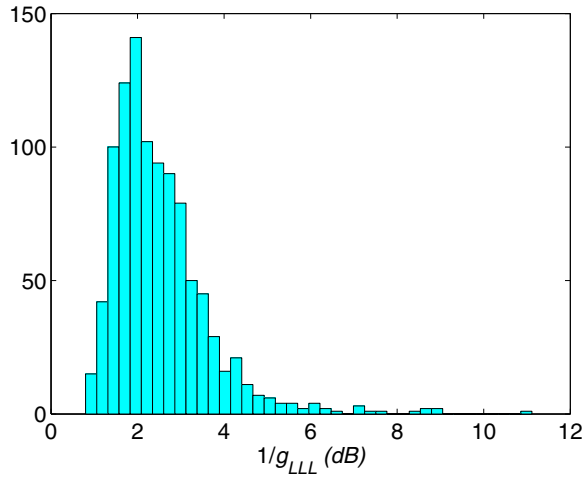

Fig. 4. Histogram of the values of $1/g_{\mathrm{LLL}}$.

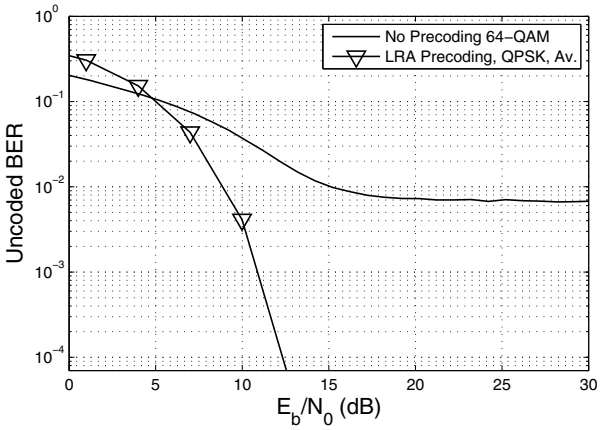

Fig. 5. SNR degradation for an 'average' interference matrix $\mathbf{H}_{av}$.

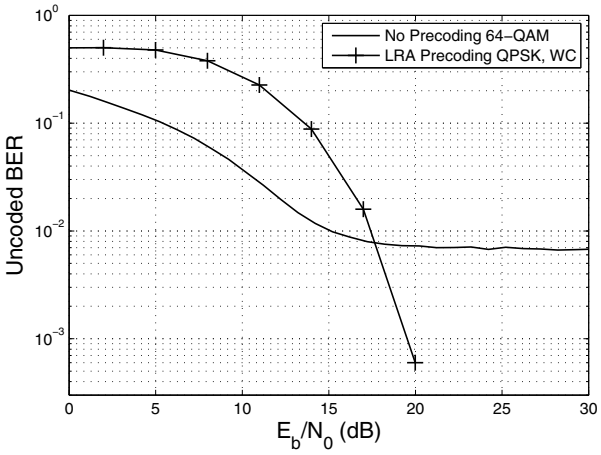

Fig. 6. SNR degradation for the worst case interference matrix $\mathbf{H}_{wc}$.

for each set of users, d_{MIN} is the minimum distance among the users' positions. This clearly indicates that d_{MIN} plays a major role in determining the performance of LRA precoding.

Let us consider the two interference matrices $\mathbf{H}_{av}$ and $\mathbf{H}_{wc}$ corresponding to a set with $\tilde{g}_{\mathrm{LLL}} \approx E\{g_{\mathrm{LLL}}\}$ and $\hat{g}_{\mathrm{LLL}} = \min g_{\mathrm{LLL}}$, respectively. Figs. 5 and 6 present the THP uncoded BER performance corresponding to a system with full frequency reuse and interference matrices $\mathbf{H}_{av}$ and $\mathbf{H}_{wc}$, respectively, compared with the performance of a system without precoding and $n_{\mathrm{C}} = 3$. Moreover, since in the last case the available bandwidth is three times higher, we compare the BER performance of 64-QAM modulation for the system without precoding and QPSK modulation for the LRA-precoded system, such that the throughput is roughly the same. Fig. 5 shows that in the average case the LRA-precoded system has better uncoded BERs for all the SNRs of interest. On the contrary, one can see in Fig. 6 that in the worst case scenario the system without precoding yields better uncoded BER performance for low SNR, suggesting that the utility of precoding strongly depends on the considered scenario. In the next Sections we will assess thoroughly the improvements and the drawbacks on the throughput coming from using LRA THP precoding.

IV. Throughput comparison

We have compared the throughput of a satellite multibeam system in the case of cluster size $n_{\mathrm{C}} = 3$, when the precoding is not necessary, and in the case $n_{\mathrm{C}} = 1$, where THP allows the elimination of CCI without degrading too much the SNR. This last scenario allows the exploitation of a bandwidth three times higher, even if a greater bandwidth corresponds to a higher noise power, as we will discuss later on.

It is worth noting that despite the little CCI obtained by the usage of clusters, at high SNR the BER of a system without any form of CCI cancellation reaches a floor which is determined by the interference power. In order to obtain a better exploitation of the capacity of the channel, systems like DVB-S2 provide for Adaptive Coding and Modulation (ACM) [19]. For example, the DVB-S2 standard defines the SNR intervals for each different Transmission Mode (TM) and provides the corresponding spectral efficiency. For the higher TMs the BER floor caused by the interference can be relevant (see the 64-QAM BER curve in Figs. 5 and 6) and the real spectral efficiency in the presence of CCI can be significantly different from the expected one. Indeed, it is possible that for certain values of the interference the highest TMs cannot be employed.

Noteworthy, it would be easy to derive the Signal to Noise and Interference Ratio (SNIR) for each receiver from the knowledge of the interference matrix $\mathbf{H}$. However, the BER performance for a given SNIR does not correspond to that obtained with an equivalent SNR, because the interference is not Gaussian as the noise. For this reason, we have to resort to simulation to assess the BER performance of a system with CCI. Moreover, also in the case of perfect (ZF) elimination of the CCI, the noise seen by the receiver is not Gaussian because of the modulo operation, and thus the coded BER is in general different from the AWGN scenario [8]. Consequently, even if we can readily determine the SNR gap due to the precoding, as shown in sec. II.C, we have in general to obtain the *coded* BER also by simulation.

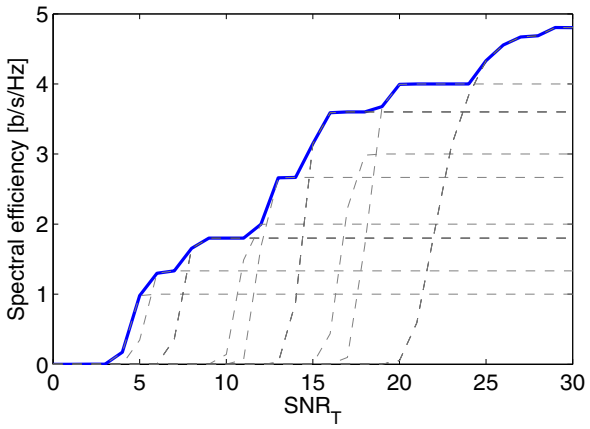

Fig. 7. Spectral efficiency for the cluster size 3 scenario.

Since we are not interested in assessing the exact performance of DVB-S2, while we just aim to compare the throughput of THP and $n_{\mathrm{C}} = 1$ with no precoding and $n_{\mathrm{C}} = 3$, we do not employ herein the DVB-S2 ACM definition by resorting to a much simpler ACM scheme, which can ensure a good exploitation of the capacity of the channel without requiring excessively long simulations. We have defined a custom ACM scheme based on three modulations: QPSK, 16-QAM and 64-QAM; and on five BCH codes with code-rates 1/4, 1/2, 2/3, 3/4 and 9/10 and codeword length 1024 bits. The information bits per codeword and the correction capabilities are 258, 513, 688, 778 and 923, and 106, 57, 37, 25 and 10, respectively.

Fig. 7 is an example to show how we derive the throughput of a system without precoding and with cluster size $n_{\mathrm{C}} = 3$: we calculate the throughput for all the modulations and all the code-rates and then, for each SNR, we select the ACM mode with the highest throughput.

Using this ACM scheme, we compared the throughput of three systems corresponding to the clusterings shown in Figs. 1 and 2. The first one is characterized by a cluster size $n_{\mathrm{C}} = 3$, as shown in Fig. 2, in order to reduce the CCI, and thus does not employ any precoding, while the other two systems exploit LRA THP to eliminate CCI and allow a full frequency reuse, i.e., cluster size $n_{\mathrm{C}} = 1$, as shown in Fig. 1. Specifically, we consider an 'average' placement of the users in the 10 beams of Fig. 1, corresponding to the interference matrix $\mathbf{H}_{av}$ defined in Section III and the worst case placement shown in Fig. 1 that corresponds to the matrix $\mathbf{H}_{wc}$.

Fig. 8 plots the throughput of the systems as a function of the SNR *at the transmitter* that is defined $\mathrm{SNR}_T = P_T/(BN_0)$, where P_T is the transmitted power of the satellite gateway, while the bandwidth is either $B = 10$ Mhz or $B = 30$ Mhz for cluster size $n_{\mathrm{C}} = 3$ and $n_{\mathrm{C}} = 1$, respectively.

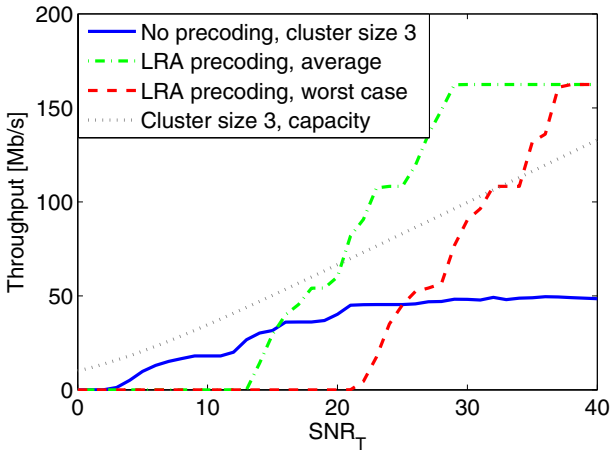

Fig. 8. Throughput for different scenarios.

Consequently, when the same ACM mode is employed, the throughput at saturation is three times higher for the case $n_C = 1$. Thus, if the ACM scheme is fixed, precoding brings a big advantage at high SNR_T values.

It can be observed in Fig. 8 that the throughput of a system with full frequency reuse and an "average" value of the inter-beam interference (employing precoding) clearly outperforms a system with cluster size $n_C = 3$ (and no precoding) for SNR_T values bigger than 14 dB. It is difficult to give general statements for SNR_T values higher than 20 dB, since higher order modulations were not enabled for the system with $n_C = 3$; however if the ACM scheme is assumed to be fixed for both systems, then precoding with $n_C = 1$ again outperforms $n_C = 3$ with no precoding also in this region. On the other hand, Fig. 8 shows that, for SNR_T higher than 20 dB, LRA THP with 'average' CCI achieves a throughput that exceed the channel capacity of the system with $n_C = 3$. Moreover, the gap between the capacity of the two systems clearly increases with SNR_T. Anyway a deeper analysis of this case is left for future works. Conversely, in the case of bad inter-beam interference ("worst case") the throughput curve of the system with $n_C = 1$ is shifted by almost 9 dB and it becomes higher than the $n_C = 3$ case only for very high SNR_T values, which makes it not very viable. In this respect it is worth noting that the system without precoding has a more than 5 dB advantage on the two $n_C = 1$ scenarios which comes from the fact that the system works on a bandwidth three times smaller and consequently faces a noise which is three times less powerful.

V. Conclusion

We have shown in this paper that, by exploiting the MIMO structure of multibeam satellite channels, DPC techniques (such as Tomlinson-Harashima Precoding) can be successfully applied. The use of such a precoding technique makes sense only in situations of intermediate inter-beam interference, when the positions of simultaneous users on the ground (located in the different beams) induce a particular structure of the interference matrix $\mathbf{H}$. We have also highligted how this apparently complex interference level's dependence on the users positions can be simply modelled by a single parameter obtained by an opportune factorization of the interference matrix $\mathbf{H}$. The values of such a parameter can be used to better exploit the frequency reuse in the satellite beams and to boost the overall system capacity.

Acknowledgment

This work was partially funded by the European Commission with the Satellite communications Network of Excellence (SatNEx), in the 6th Framework Programme, contract No. IST-27393. The authors would like to thank Marcos Alvarez Diaz and Gianluigi Liva for their precious suggestions that improved a lot the final quality of this work.

References

[1] E. Lutz, M. Werner, and A. Jahn, *Satellite Systems for Personal and Broadband Communications*, 1st ed. Springer-Verlag, 2000.
[2] D. Gesbert, M. Shafi, D. shan Shiu, P. Smith, and A. Naguib, "From theory to practice: an overview of MIMO space-time coded wireless systems," *Selected Areas in Communications, IEEE Journal on*, vol. 21, no. 3, pp. 281–302, Apr 2003.
[3] Q. Spencer, C. Peel, A. Swindlehurst, and M. Haardt, "An introduction to the multi-user MIMO downlink," *IEEE Commun. Magazine*, vol. 42, no. 10, pp. 60–67, Oct. 2004.
[4] B. Beidas, H. El Gamal, and S. Kay, "Iterative interference cancellation for high spectral efficiency satellite communications," *IEEE Trans. Commun.*, vol. 50, no. 1, pp. 31–36, Jan 2002.
[5] R. F. H. Fisher, *Precoding and Signal Shaping for Digital Transmission*. New York: Wiley-IEEE Press, July 2002.
[6] M. H. M. Costa, "Writing on dirty paper," *IEEE Trans. Inform. Theory*, vol. 29, pp. 439–441, May 1983.
[7] M. Joham, W. Utschick, and J. Nossek, "Linear transmit processing in MIMO communications systems," *IEEE Trans. Signal Process.*, vol. 53, no. 8, pp. 2700–2712, Aug. 2005.
[8] R. F. H. Fisher, "Comparison of precoding schemes for digital subscriber lines," *IEEE Trans. Commun.*, vol. 45, pp. 334–343, Mar. 1997.
[9] M. Diaz, N. Courville, C. Mosquera, G. Liva, and G. Corazza, "Non-linear interference mitigation for broadband multimedia satellite systems," *IWSSC '07*, pp. 61–65, Sept. 2007.
[10] C. Haardt and N. Courville, "Internet switching by satellite: an ultra fast proscessor with radio burst switching," in *Proc. Disruption in Space*, Marseille, France, 4-6 July 2005.
[11] M. Tomlinson, "New automatic equalizer employing modulo arithmetic," *IEE Electronic Letters*, vol. 7, pp. 130–139, Mar. 1971.
[12] H. Harashima and H. Miyakawa, "Matched transmission technique for channels with intersymbol interference," *IEEE Trans. Commun.*, vol. 20, pp. 774–780, Aug. 1972.
[13] L. Sanguinetti and M. Morelli, "Non-linear pre-coding for multiple-antenna multi-user downlink transmissions with different QoS requirements," *IEEE Trans. Wireless Commun.*, vol. 6, pp. 852–856, Mar. 2007.
[14] R. Muller, D. Guo, and A. L. Moustakas, "Vector precoding for wireless MIMO systems and its replica analysis," *IEEE J. Select. Areas Commun.*, vol. 26, pp. 530–540, Apr. 2008.
[15] C. Windpassinger, R. F. H. Fisher, and J. Huber, "Lattice-reduction-aided broadcast precoding," *IEEE Trans. Commun.*, vol. 52, pp. 2057–2060, Dec. 2004.
[16] A. K. Lenstra, H. W. Lenstra, and L. Lovasz, "Factoring polynomials with rational coefficients," *Math. Ann.*, vol. 261, p. 515534, 1982.
[17] C.-H. F. Fung, W. Yu, and T. J. Lim, "Precoding for the multiantenna downlink: Multiuser SNR gap and optimal user ordering," *IEEE Trans. Commun.*, vol. 55, p. 188197, Jan. 2007.
[18] J. G. Proakis, *Digital Communications*, 4th ed. McGraw-Hill, 2001.
[19] ETSI, *EN 302 307 - V1.1.2*, 2006.